AD 402 616

DOC. NO.
NARF-62-13T
MR-N-297

A MONTE CARLO MULTIBEND DUCT PROCEDURE

U S A F

NUCLEAR AEROSPACE RESEARCH FACILITY

operated by

GENERAL DYNAMICS | FORT WORTH

DOC. NO.
NARF-62-13T
MR-N-297

DOC. NO.
NARF-62-13T
MR-N-297

USAF

NUCLEAR AEROSPACE RESEARCH FACILITY

15 SEPTEMBER 1962

A MONTE CARLO MULTIBEND DUCT PROCEDURE

D. G. COLLINS

CONTRACT
AF 33(657)-7201

SECTION II, TASK I,
ITEM 8 OF FZM-2386

ISSUED BY THE
ENGINEERING
DEPARTMENT

GENERAL DYNAMICS | FORT WORTH

ABSTRACT

A Monte Carlo procedure was developed to evaluate the energy, angular distribution, and intensity of either the scattered neutron or gamma-ray flux that penetrates a multibend duct. The procedure has been coded for the IBM 7090.

A detailed presentation of the Monte Carlo method as an approximation to the Neumann series solution of the integral transport equation is given. Sampling techniques utilized by the procedure are described. Included in these techniques are splitting, Russian Roulette, statistical estimation, and a method of biasing the sampling from the source angular distributions.

Results obtained with the procedure are compared with the data taken in the duct penetration and systemization experiment conducted at General Dynamics/Fort Worth. This comparison confirms the validity of the methods. Further, it shows that the procedure will be a valuable aid in the analysis of experimental data as well as in the determination of the validity and range of applicability of some of the simpler methods developed to calculate the flux penetrating a multibend duct.

REPORT SUMMARY

Due to the success of a recent application of the Monte Carlo method to problems involving neutron scattering and penetration through straight cylindrical ducts, it was decided to modify the procedure so that multibend ducts might be considered. Routines providing for the treatment of gamma-ray scattering and for the use of splitting and Russian Roulette techniques were also added to the procedure. One of the greatest assets of the procedure is that a rigorous treatment of multiple scattering within a multibend-duct configuration is possible. A neutron or gamma-ray source may be described with a set of from 1 to 30 point sources. The energy and angular distribution and the intensity of the scattered flux are calculated for each of a set of from 1 to 30 detector points. The unscattered flux is also calculated for each detector position and recorded separately so that the total flux as well as the relative contributions from scattered and unscattered radiation may be determined.

The Monte Carlo method is presented as an approximation of the Neumann series solution of the integral transport equation. A discussion of the method developed to bias the sampling from the source angular distributions is given, and a description of the Russian Roulette and splitting techniques utilized by the procedure is presented.

A comparison of results obtained with the procedure and from experimental data taken in the duct systemization study is shown to confirm the validity of the procedure.

The ability of the procedure to treat multiple scattering rigorously and the versatility offered by the procedure in geometric description allow a fairly accurate analysis of neutron and gamma-ray radiation streaming through a multibend duct. Use of the procedure should lead to a more confident prediction of the flux streaming through multibend ducts than has been obtainable with some of the less exacting methods.

TABLE OF CONTENTS

LIST OF FIGURES

LIST OF TABLES

I. INTRODUCTION

The methods presently available for calculating the amount of radiation that penetrates a multibend duct lack the versatility that is necessary to give a complete analysis of the multiple scattering which is certain, in many geometric configurations, to be responsible for a significant portion of the flux penetrating the duct. Two of the methods most commonly used - the single-scattering method and the albedo method - are described in Reference 1. These methods have given good results for a certain class of duct configurations, namely, those that have a high length-to-diameter ratio. As pointed out in Reference 1, however, these methods have failed to predict experimental data for ducts with low length-to-diameter ratios. In References 2 and 3, applications of diffusion theory to the problem of radiation penetrating shields containing multibend ducts are described, but the developments of the theory are not supported by experimental data.

Because of the success of a recent application of the Monte Carlo method to problems involving the scattering of neutrons and their penetration through straight cylindrical ducts (Ref. 4), it was decided to modify the procedure so that multibend ducts might be considered. Routines providing for the treatment of gamma-ray scattering and for the splitting and Russian Roulette techniques were also added to the procedure.

This modified version, referred to as The Multibend-Duct Procedure (LO5), has been coded for the IBM 7090 for use in the analysis of neutron or gamma-ray radiation streaming through a multibend duct. The procedure is designed to calculate the direct-beam, scattered fluxes and dose rates at from 1 to 30 detector positions at points of interest within or near a multibend-duct configuration. Print options are provided so that the energy and angular distributions of the scattered flux at each detector position may be obtained.

One of the greatest assets of this procedure is that multiple scattering within a multibend-duct geometry may be treated rigorously. The procedure allows an accurate description of most multibend ducts. It is anticipated that the multibend-duct procedure will prove to be a valuable tool in the analysis of experimental data and in determining the validity and range of applicability of some of the simpler methods developed to calculate the radiation penetrating a multibend duct.

A description of the geometry and of the Monte Carlo method utilized by the procedure is given in Section II. An evaluation of the procedure, based on comparisons of calculated and measured data, is given in Section III.

II. METHOD

The procedure involves the application of the Monte Carlo method to compute the energy and angular distributions and the intensity of the scattered neutron or gamma flux that penetrates a multibend duct. The unscattered flux is also computed and recorded separately so that the total flux at any detector point, as well as the magnitudes of the scattered and unscattered flux, may be determined. Options are provided for splitting and Russian Roulette and for biasing the source angular distributions.

2.1 Geometry and Source Description

The geometrical description of a multibend-duct configuration is accomplished in the manner described in this subsection. A base coordinate system is chosen with its origin lying outside of the geometry to be described (Fig. 1). The multibend-duct configuration is then divided into sections by a set of planes, so that between any two consecutive planes the duct contains no bends and has a constant diameter. Associated with the second of any two consecutive planes is a set of radii consisting of the outer radii of each cylindrical shell region between the two planes. In tracking particles as they scatter through this geometry, a double subscript is used to identify the regions; for instance, Σ_{pi} would be the macroscopic cross section for the ith cylindrical region associated with the pth plane. In the base coordinate system, the pth plane is defined by the point of intersection (X_p, Y_p, Z_p) of the plane and its normal.

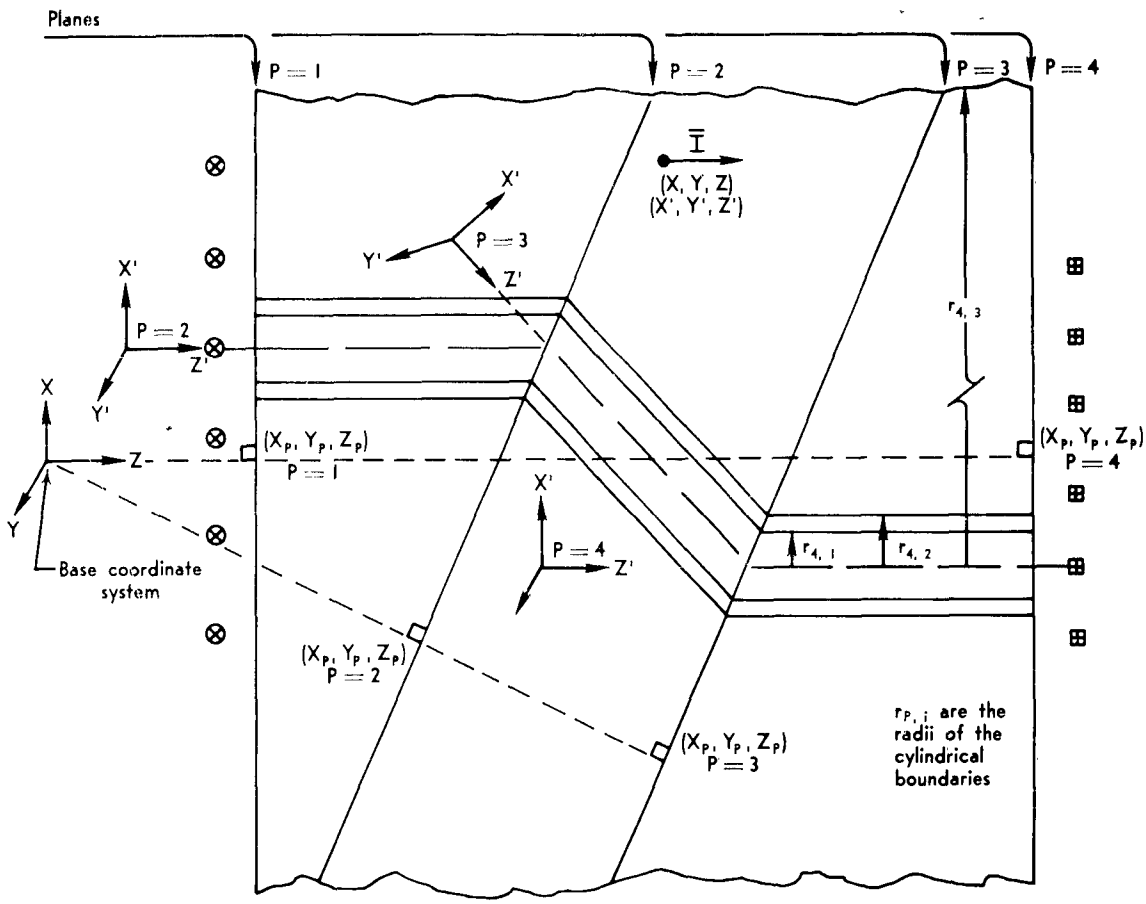

1. Planes are identified by a single point (X_p, Y_p, Z_p) in the base coordinate system
2. Coordinates of source points, ⊗, and detector points, ⊞, must be given in terms of the base coordinate system
3. Beginning with the second plane, a set of 3 vectors $(\bar{A}, \bar{B}, \bar{C})$ is input to describe the transformation from the base coordinate system to the prime coordinate system that has the Z' axis coincident with the axis of the duct on the origin side of the plane (see Fig. 2)

Figure 1. Multibend Duct Geometry

A prime coordinate system is also associated with each plane (beginning with the second). The Z' axis of this system is coincident with the line of symmetry of the regions between the two consecutive planes. The transformation from the base coordinate system to the prime coordinate system is accomplished by three vectors: $\bar{A} = a_1, a_2, a_3$, the vector to the origin of the prime coordinate system; $\bar{B} = b_1, b_2, b_3$, the vector to the point (0, 0, 10) in the prime coordinate system; and $\bar{C} = c_1, c_2, c_3$, a vector to the point (10, 0, 0) in the prime coordinate system. Therefore, the relationship between a point (X', Y', Z') in the prime coordinate system and the same point (X, Y, Z) in the base system is as follows:

Letting $\bar{X} = X, Y, Z$ be a vector to the point (X, Y, Z),

then
$$X' = \frac{(\bar{X} - \bar{A}) \cdot (\bar{C} - \bar{A})}{10},$$

$$Y' = \frac{(\bar{X} - \bar{A}) \cdot \left[(\bar{B} - \bar{A}) \times (\bar{C} - \bar{A})\right]}{100},$$

and
$$Z' = \frac{(\bar{X} - \bar{A}) \cdot (\bar{B} - \bar{A})}{10}.$$

The angles k' and ϕ', which define the particles direction at the point (X, Y, Z) or (X', Y', Z'), are given by

$$k' = \cos^{-1}\left[\frac{(\bar{B} - \bar{A}) \cdot \bar{I}}{|\bar{B} - \bar{A}|}\right],$$

$$\cos \phi' = \frac{(\bar{C} - \bar{A}) \cdot \bar{I}}{|\bar{C} - \bar{A}| \sin k'}, \text{ and}$$

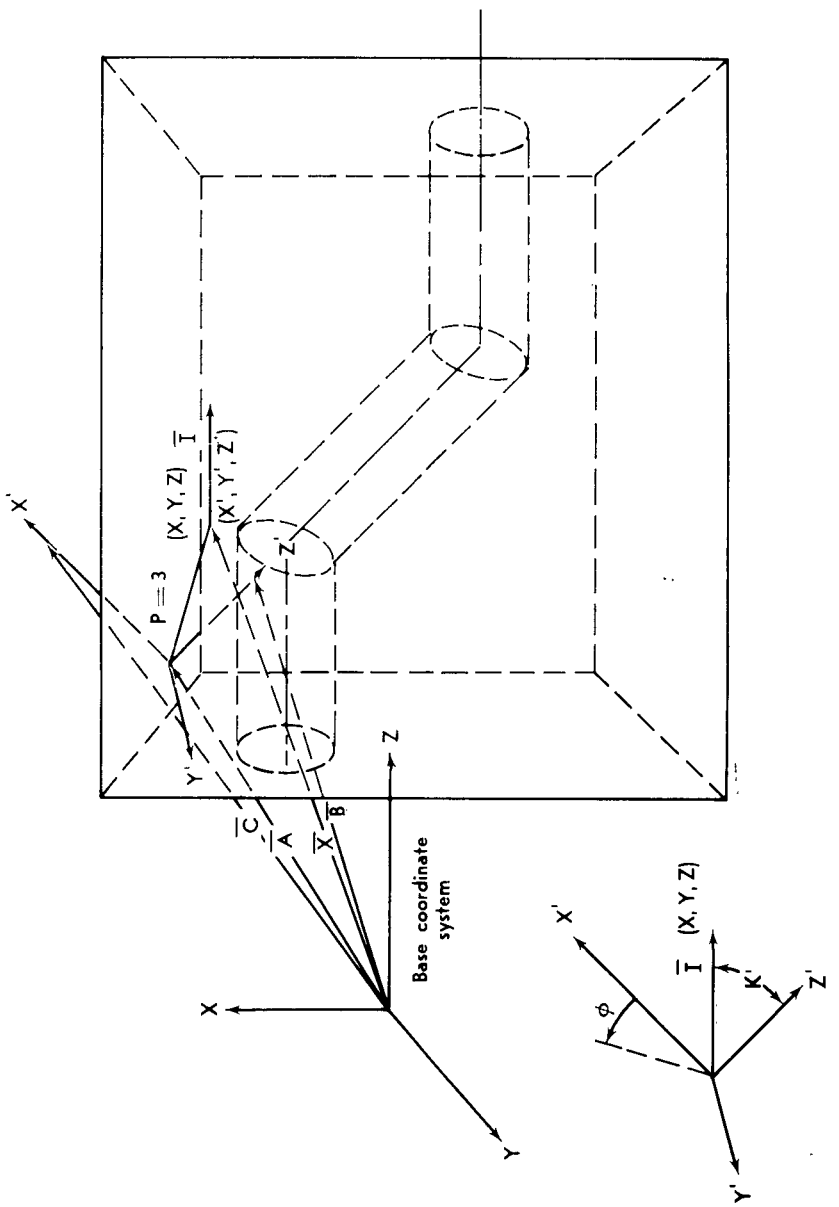

Figure 2. Transformation of Coordinate System

$$\sin \phi' = \frac{\left[(\bar{B} - \bar{A}) \times (\bar{C} - \bar{A})\right] \cdot \bar{I}}{\left|(\bar{B} - \bar{A}) \times (\bar{C} - \bar{A})\right| \sin k'} ,$$

where $\bar{I}$ is a unit vector in the direction of the particle.

A set of from 1 to 30 source points may be used to approximate a neutron or gamma-ray source. The source energy may be monoenergetic or an arbitrary spectrum, but the spectrum must be the same for all source points. There may be a different angular distribution for each source point, and a different importance function may be used to sample from each of the angular distributions.

2.2 Scattering Theory

The Monte Carlo method has, in general, been considered as a method of solving integral equations. The method lends itself well to those multiple integrals that have their limits complicated by the boundary conditions imposed. Thus, it has been used quite extensively in the solution of neutron and gamma-ray transport problems involving complex geometries.

The method, as presented here, approximates the Neumann series solution of the integral transport equation:

$$F(\bar{R}) = \sum_{n=o}^{\infty} I_n (\bar{R}),$$

where $F(\bar{R})$ represents the total flux at detector position $\bar{R}$, and $I_n(\bar{R})$ is the contribution to the flux from the nth order of scattering.

If the series $F(\bar{R})$ converges, it may be approximated by

$$F(\bar{R}) = \sum_{n=0}^{n_{max}} I_n(\bar{R}), \tag{1}$$

where the sum of the contributions to the flux from orders of scattering above n_{max} is negligible when compared to the sum of the contributions from orders of scattering less than or equal to n_{max}.

The direct beam, or unscattered flux, at position $\bar{R}$ is given by the first term of the series,

$$I_c(\bar{R}) = \frac{S(\bar{R}_o, \bar{\Omega}_o, E_o)}{|\bar{R}-\bar{R}_o|^2} \exp\left[- \int_0^{\bar{\Omega}_o' \cdot (\bar{R}-\bar{R}_o)} \Sigma_T(\bar{R}_o + S\bar{\Omega}', E_o)\, ds \right] \delta(\bar{\Omega}'-\bar{\Omega}_o),$$

where $S(\bar{R}_o, \bar{\Omega}_o, E_o)$ is the source strength at the position $\bar{R}_o$ expressed in the terms of neutrons per second per steradian in the direction $\bar{\Omega}_o$ with energy E_o,

$\delta(\bar{\Omega}'-\bar{\Omega}_o)$ is the Dirac delta function, and

$\bar{\Omega}'$ is a unit vector in the direction $R-R_o$.

The integral expression

$$\int_0^{\bar{\Omega}' \cdot (\bar{R}-\bar{R}_o)} \Sigma_T(\bar{R}_o + S\bar{\Omega}', E_o)\, ds$$

represents the number of mean-free-path lengths between $\bar{R}_o$ and $\bar{R}$ and is written in this form to indicate that the macroscopic cross section, Σ_T, is a function of position.

The first term of the series, $I_o(R)$, may be determined exactly, but the rest of the terms are approximated by the Monte Carlo method. A monoenergetic point source will be assumed for the presentation of the method. The single-scattered flux is then represented by

$$I_1(\bar{R}) = \int \frac{S(\bar{R}_o,\bar{\Omega}_o,E_o)}{|\bar{R}_1-\bar{R}_o|^2}\,\Sigma_T(\bar{R}_1,E_o)\,\exp\left[-\int_o^{\bar{\Omega}_o\cdot(\bar{R}_1-\bar{R}_o)}\Sigma_T(\bar{R}_o+s\bar{\Omega}_o,E_o)\,ds\right]$$

$$W(\bar{R}_1,E_o)\,f(\bar{\Omega}_o,E_o\longrightarrow\bar{\Omega}',\bar{E}')\,\exp\left[-\int_0^{\bar{\Omega}'\cdot(\bar{R}-\bar{R}_1)}\Sigma_T(\bar{R}_1+s\bar{\Omega}',E')\,ds\right]\frac{d\bar{R}_1}{|\bar{R}-\bar{R}_1|^2}\ ,$$

where $\Sigma_T(\bar{R}_1,E_o)$ is the macroscopic total cross section at position $\bar{R}_1$ and at energy E_o,

$W(\bar{R}_1,E_o) = \dfrac{\Sigma_s(\bar{R}_1,E_o)}{\Sigma_T(\bar{R}_1,E_o)}$ is the ratio of the macroscopic scattering to the macroscopic total cross section at position $\bar{R}_1$ and energy E_o,

$f(\bar{\Omega}_o,E_o\longrightarrow\bar{\Omega}',E')$ is the probability density function* for scattering from direction $\bar{\Omega}_{n-1}$ to $\bar{\Omega}_n$, and

$$d\bar{R}_1 = R_1^{\,2}\sin k_o\,dk_o\,d\phi_o\,dR_1,$$

where $R_1 = |\bar{R}_1-\bar{R}_o|$,

k_o is the polar angle in the direction $\bar{\Omega}_o$, and

ϕ_o is the azimuthal angle in the direction $\bar{\Omega}_o$.

---

*A detailed discussion of this function along with methods of sampling scattering angles from the function is given in Section 2.3 of this report.

In general, for $n \geq 1$,

$$I_n(\bar{R}) = \int \cdots \int S(\bar{R}_o, \bar{\Omega}_o, E_o)\, K(\bar{R}_{n-1}, \bar{R}_n)\, W(\bar{R}_n, E_{n-1})$$

$$E_n(\bar{R}, \bar{\Omega}', E')\, d\bar{R}_n \cdots\cdots d\bar{R}_1, \tag{2}$$

where

$$K(\bar{R}_{n-1}, \bar{R}_n) = \prod_{i=0}^{n-1} \Sigma_T(\bar{R}_{i+1}, E_i) \exp\left[- \int_0^{\bar{\Omega}_i \cdot (\bar{R}_{i+1} - \bar{R}_i)} \Sigma_T(\bar{R}_i + s\bar{\Omega}_i, E_i)\, ds \right]$$

$$f(\bar{\Omega}_{i-1}, E_{i-1} \longrightarrow \bar{\Omega}_i, E_i)\, \frac{1}{|\bar{R}_{i+1} - \bar{R}_i|^2} \tag{3}$$

with

$$f(\bar{\Omega}_{-1}, E_{-1} \longrightarrow \bar{\Omega}_o, E_o) = 1 \text{ for } i = 0,$$

$$W(\bar{R}_n, E_{n-1}) = \prod_{i=1}^{n} \frac{\Sigma_s(\bar{R}_i, E_{i-1})}{\Sigma_T(\bar{R}_i, E_{i-1})}\,, \tag{4}$$

and

$$E_n(\bar{R},\ \bar{\Omega}',\ E') = \exp\left[- \int_0^{\bar{\Omega}' \cdot (\bar{R} - \bar{R}_n)} \Sigma_T(\bar{R}_n + S\ \bar{\Omega}',\ E')\ ds \right]$$

$$f(\ \bar{\Omega}_{n-1},\ E_{n-1} \longrightarrow \bar{\Omega}',\ E') \frac{1}{|\ \bar{R} - \bar{R}_n\ |^2} \cdot \qquad (5)$$

The Monte Carlo method utilized in approximating Equation 1 is a history-generating process whereby each history gives an estimate of each term of the series but the first, and thus generates an estimate of the scattered flux. One history is the process of sampling path lengths and scattering angles from the expressions $K(\bar{R}_{n-1},\ \bar{R}_n)$ and evaluating the estimators $E_n(\bar{R},\ \bar{\Omega}',\ E')$ and $W\ (\bar{R}_n,\ E_{n-1})$ for all but the first term of the series. It will be noticed that

$$K(\bar{R}_{n-1},\ \bar{R}_n) = K(\bar{R}_{n-2},\ \bar{R}_{n-1})\ \Sigma_T(\bar{R}_n,\ E_{n-1})$$

$$\exp\left[- \int_0^{\bar{\Omega}_{n-1} \cdot (\bar{R}_n - \bar{R}_{n-1})} \Sigma_T(\bar{R}_{n-1} + S\ \bar{\Omega}_{n-1},\ E_{n-1})\ ds \right]$$

$$f(\ \bar{\Omega}_{n-2},\ E_{n-2} \longrightarrow \bar{\Omega}_{n-1},\ E_{n-1})\ ,$$

so that the position of the nth collision is dependent upon the position of the n-1st collision. Thus, samples drawn from

$K(\bar{R}_{n-2}, \bar{R}_{n-1})$ to obtain an estimate of $I_{n-1}(\bar{R})$ may be reused in obtaining an estimate of $I_n(\bar{R})$.

Evaluating the expressions $E_n(\bar{R}, \bar{\Omega}', E')$ and $W(\bar{R}_n, E_{n-1})$ for the values of $\bar{R}_i$ sampled from $K(\bar{R}_{n-1}, \bar{R}_n)$ gives an estimate of the magnitude of the flux at $\bar{R}$, which has direction $\bar{\Omega}'$ and energy E'. Therefore, by allocating storage locations for energy and angle groups, an estimate may be added into the proper groups; and, after a sufficient number of histories are processed, histograms of the energy and angular distributions of the scattered flux can be determined. Estimates of the total-scattered flux at $\bar{R}$, $S_i(\bar{R})$ are obtained by adding the estimates from each order of scattering.

The final estimate of the scattered flux at a position $\bar{R}$ is taken to be the average value of the estimates obtained from the individual histories:

$$S(\bar{R}) = \frac{1}{H} \sum_{i=1}^{H} S_i(\bar{R}) ,$$

where $S(\bar{R})$ is the scattered flux at the position $\bar{R}$, as estimated by the Monte Carlo method, and $S_i(\bar{R})$ represents the estimates of the scattered flux obtained from the individual histories. An estimate of the variance of the fluxes from the individual histories is given by

$$V\left[S(\bar{R})\right] = \frac{\sum_{i=1}^{H} \left[S_i(\bar{R})\right]^2}{H} - \frac{\left[\sum_{i=1}^{H} S_i(\bar{R})\right]^2}{H^2} .$$

When a sufficient number of histories have been processed,

$$S(\bar{R}) \cong \sum_{n=1}^{n_{max}} I_n(\bar{R})$$

and

$$I_o(\bar{R}) + S(\bar{R}) \cong F(\bar{R}).$$

2.3 Sampling Methods

In the Monte Carlo method utilized by this procedure, path lengths and scattering angles are chosen by a random process to obtain the distribution of the collision points in a geometric configuration containing a multibend duct. The concept of weighting is also introduced to allow sampling from other than the actual physical distributions of source angles and collision densities, and to adjust for the fact that no absorption collisions are allowed.

A method of biasing the sampling from the angular distribution of a point-isotropic or a point-anisotropic source was developed so that those angles which give the source particle a higher probability of reaching the detector may be given more emphasis than they would ordinarily receive in straightforward sampling. For this biased sampling scheme, the unit sphere about the source point is divided into areas which may be unequal in size but are considered to be of equal importance. The divisions in area are

made with respect to the polar angle, giving I angle sectors that are bounded by I - 1 polar angles. Each sector is considered to be of equal importance, so that the total number of histories to be run are divided equally among the sectors. The adjustment to the weighting factor for the ith vector to remove the bias introduced by the sampling process is

$$W_i = I \left\{ \frac{\int_{k_{i-1}}^{k_i} n(\theta) \sin \theta d\theta}{\int_0^{\pi} n(\theta) \sin \theta d\theta} \right\}, \qquad (6)$$

where I is the total number of sectors, k_{i-1} and k_i are the polar angles bounding the ith sector, and $n(\theta)$ is the angular density function describing the angular distribution of particles emitted from the source.

The cosines of the polar angles defining the sectors are listed as input for the procedure, and the weighting factors of each sector are listed when the angular distribution is anisotropic. For the case of an isotropic distribution, the weight adjustment factors are calculated by the machine by use of Equation (6), which reduces to

$$W_i = I \left[\frac{\cos k_{i-1} - \cos k_i}{2} \right],$$

when $n(\theta)$ is the isotropic distribution.

The path lengths, $R_i = |\bar{R}_i - \bar{R}_{i-1}|$, are sampled from the distribution function

$$RN = \int_0^{r_i} \Sigma_T(\bar{R}_i, E_{i-1}) \exp\left[-\int_0^{\bar{\Omega}_{i-1} \cdot (\bar{R}_i - R_{i-1})} \Sigma_T(\bar{R}_{i-1} \quad S\bar{\Omega}_{i-1}, E_{i-1})\, ds\right] dR_i,$$

where RN is a random number, and

$$\Sigma_T(\bar{R}_i, E_{i-1}) \exp\left[-\int_0^{\bar{\Omega}_{i-1} \cdot (\bar{R}_i - \bar{R}_{i-1})} \Sigma_T(\bar{R}_{i-1} \quad S\bar{\Omega}_{i-1}, E_{i-1})\, ds\right]$$

is one of the integral expressions given in Equation 3. $\bar{R}_i = \bar{R}_{i-1} + R_i\bar{\Omega}_{i-1}$ gives the position of the ith collision. After determining the position of each collision, the weighting function is multiplied by $\Sigma_S(\bar{R}_i, E_{i-1})/\Sigma_T(\bar{R}_i, E_{i-1})$, since only scattering collisions are allowed. From each collision point an estimate of the flux reaching each of the detector points is made, assuming that no further collisions occur between that point and the detectors. The estimating function is

$$W(\bar{R}_n, E_{n-1})\, E_n(\bar{R}, \bar{\Omega}', E'),$$

as given in Equations 4 and 5.

A close examination of the expression

$$\exp\left[-\int_0^{\bar{\Omega}' \cdot (\bar{R} - \bar{R}_n)} \Sigma_T(\bar{R}_n + S\bar{\Omega}', E')\, ds\right],$$

contained within $E_n(\bar{R},\bar{\Omega}',E')$, reveals that collisions occurring near a detector point will contribute much more to the scattered flux than those occurring farther away. This being the case, it is advisable to ensure that a sufficient number of collisions are sampled in those areas near the detector. In order to improve the sampling of collisions in areas near a detector, an option providing for the splitting and Russian Roulette techniques is included within the procedure. Splitting and Russian Roulette result in a change in the number of particles being followed. Consequently, the particle weights must be correctly adjusted to eliminate the bias introduced by these techniques. The option requires that a splitting factor, M, and a set of splitting boundaries, H_B, be listed as input. The factor, M, is an integer and determines the number of particles into which a single particle will be split or the number of particles that will be combined into one particle upon crossing a splitting boundary. The splitting boundaries H_1, H_2, ... H_B, ... H_{max} are listed in ascending order and define the loci of points lying H_1, H_2, ... H_B, ..., H_{max} relaxation lengths from the detector point. The quantity

$$H = \int_0^{\bar{\Omega}' \cdot (\bar{R} - \bar{R}_n)} \Sigma_T(\bar{R}_n + S\bar{\Omega}', E')ds$$

in Equation 5 gives the number of relaxation lengths between the nth collision point and the detector; therefore B, the index of the

largest value of $H_B < H$, is the number of splitting boundaries between the nth collision point and the detector. If B' and B are the number of splitting boundaries between the detector point and the n-1st and the nth collision point, respectively, then $|B'-B|$ is the number of splitting boundaries that a particle crosses in going from the n-1st to the nth collision point. If $B' > B$, the particle is moving toward the detector and splitting occurs. In this case, the particle is split into $M^{B'-B}$ particles, so that the weight of each particle becomes

$$W_{n-1} = W'_{n-1} M^{B-B'} ,$$

where W'_{n-1} was the weight of the original particle before splitting. If $B' < B$, the particle is moving away from the detector and the Russian Roulette technique is applied. A random number, RN, is generated, and if $RN > (\frac{1}{M})^{B-B'}$, the tracking of the particle is terminated; but if $RN \leq (\frac{1}{M})^{B-B'}$, the weight W_{n-1} is multiplied by $(M)^{B-B'}$ and tracking of the particle is continued. A proper selection of the splitting factor and a proper placement of the splitting boundaries should improve the sampling of the collision points in the areas near the detector.

After an estimate of the flux reaching each detector from the nth collision has been made, the procedure returns to the location of the nth collision to choose a scattering angle,
$\psi = \cos^{-1}(\bar{\Omega}_n \cdot \bar{\Omega}_{n-1})$.

For gamma rays, the scattering angle is chosen from the Klein-Nishina differential scattering cross section for Compton scattering or from an isotropic distribution for the pair-production process. The pair-production process is assumed to be a scattering process in which two 0.50-Mev photons are given off in opposite directions. The procedure chooses the scattering process by comparing a random number with the ratio of the Compton-scattering cross section to the sum of the Compton-scattering and pair-production cross sections.

$$RN \sim \frac{\rho_e(\bar{R}_n)\ \mu_c(E_{n-1})}{\rho_e(\bar{R}_n)\ \mu_c(E_{n-1}) - \sum_j \rho_j(\bar{R}_n)\,\mu_{pp}(j, E_{n-1})},$$

where $\rho_e(\bar{R}_n)$ is the electron density at the position $\bar{R}_n$, $\mu_c(E_{n-1})$ is the Compton-scattering cross section, $\rho_j(\bar{R}_N)$ is the atomic density of the element j at the position $\bar{R}_n$, and $\mu_{pp}(j, E_{n-1})$ is the pair-production cross section for element j. The summation is over all elements j at the position $\bar{R}_n$. If RN is less than or equal to the right-hand member of Equation 6, the scattering process is taken to be Compton scattering. If RN is greater than the right-hand member of Equation 6, the scattering process is taken to be the pair-production process. The angular distribution of the photons produced by the pair-production process is assumed to be isotropic in the laboratory system, so that ψ, the polar angle of emission with respect to

the previous direction of flight $\bar{\Omega}_{n-1}$, is given by the following equation:

$$\psi = \cos^{-1}(2RN-1),$$

where RN is a random number. To prevent the tracing of individual histories for both of the photons given by the pair-production process, both photons are assumed to be emitted in the same direction and are combined into one photon having twice the weight of the original photon. The bias introduced by assuming that both photons are emitted in the same direction will automatically be eliminated by running a large number of histories.

Sampling of the scattering angle from the Klein-Nishina differential scattering cross section for Compton-scattered photons is done by the rejection technique described on the bottom of page 65 in Reference 5.

For neutrons, the sampling of the scattering angle involves, first, a choice of the target element and, then, a choice between the elastic-and inelastic-scattering processes for that element. The target element j is selected so that

$$\sum_{k=1}^{j-1} \frac{\rho_k(\bar{R}_n)\,\sigma_T(k,\, E_{n-1})}{\Sigma_T(\bar{R}_n,\, E_{n-1})} < RN \leq \sum_{k=1}^{j} \frac{\rho_k(\bar{R}_n)\,\sigma_T(k,\, E_{n-1})}{\Sigma_T(\bar{R}_n,\, E_{n-1})} ,$$

where ρ_k is the atomic density of the element k at $\bar{R}_n$, $\sigma_T(k, E_{n-1})$ is the microscopic total cross section for the

element k, and $\Sigma_T(\bar{R}_n, E_{n-1})$ is the macroscopic total cross section at the position $\bar{R}_n$. The differential elastic-scattering cross section or the differential inelastic-scattering cross section for the element j is taken to be the distribution of the scattering angle ψ, depending upon whether a random number RN is less than or greater than

$$\frac{\sigma_{el}(j, E_{n-1})}{\sigma_{el}(j, E_{n-1}) + \sigma_{in}(j, E_{n-1})} .$$

The procedure assumes that the inelastic scattering process is isotropic in the center-of-mass system for all elements. The center-of-mass scattering angle, ψ', is then determined by the equation

$$\psi' = \cos^{-1}\left[2RN - 1\right]$$

and ψ, the angle in the laboratory system corresponding to ψ', is determined by

$$\psi = \cos^{-1}\left[\frac{1 + A' \cos \psi'}{(1 + 2A' \cos \psi' + A'^2)^{\frac{1}{2}}}\right],$$

where

$$A' = A_j \left[1 - \frac{(A_j + 1)\epsilon}{A_j(E_{n-1})}\right]^{\frac{1}{2}}$$

with A_j being the atomic weight of the element j and with ϵ being the excitation level of the target nucleus. The excitation levels of the target elements are selected from a table of input data listing the probabilities of exciting the various levels of the target nucleus as a function of the incident neutron energies.

Routines are included in the procedure for the choice of ψ in the special cases when the differential elastic-scattering cross section may be considered to be isotropic in the laboratory system or isotropic in the center-of-mass system. The procedure also allows for a table of input values of the quantity

$$\frac{\int_0^{\psi} \frac{d\sigma}{d\Omega} \sin \psi' \, d\psi'}{\int_0^{\pi} \frac{d\sigma}{d\Omega} \sin \psi' \, d\psi'}$$

for elastic scattering as a function of energy, angle, and element. If these tables are used, the set of values for the energy in the table nearest the energy of the incident neutron is chosen, and a linear interpolation is performed to determine the value of ψ corresponding to a random number.

Since any azimuthal angle Φ about the previous direction $\bar{\Omega}_{n-1}$ of a particle is equally probable, random values of Φ may be found by evaluating the integral in the following equation for Φ, where RN is a random variable:

$$RN = \int_0^{\Phi} \frac{d\Phi'}{2\pi}.$$

The directional vectors $\bar{\Omega}_i$ may be defined with two components: k_i, the polar angle with respect to the Z axis, and ϕ, the angle between the projection of the vector in the (x,y) plane and the x axis. The components k_n and ϕ_n of the vector $\bar{\Omega}_n$ may be determined from the scattering angles ψ, Φ, k_{n-1}, and ϕ_{n-1} by the following spherical triangle relationships:

$$k_n = \cos^{-1}\left[\cos k_{n-1} \cos\psi + \sin k_{n-1} \sin\psi \cos\Phi\right],$$

$$\cos \phi_n = \cos \phi_{n-1} \cos \Delta\phi_n - \sin\phi_{n-1} \sin\Delta\phi_n, \text{ and}$$

$$\sin \phi_n = \sin \phi_{n-1} \cos\Delta\phi_n + \cos\phi_{n-1} \sin\Delta\phi_n,$$

where

$$\cos\Delta\phi_n = \frac{\cos \psi - \cos k_{n-1} \cos k_n}{\sin k_{n-1} \sin k_n}$$

and

$$\sin\Delta\phi_n = \frac{\sin \psi \sin}{\sin k_n} .$$

III. COMPARISON WITH EXPERIMENTAL DATA

General Dynamics/Fort Worth is presently engaged in a duct systemization and penetration study (Ref. 6). Experimental data for several straight cylindrical ducts of different lengths and diameters have been obtained in support of the study, and it is planned to continue the experiments with multibend-duct configurations. A literature survey for other experimental data involving multibend ducts revealed that, of the data available, none was reported in sufficient detail to permit conclusive comparisons with Monte Carlo results.

Since the Multibend-Duct Procedure may also be applied to straight cylindrical ducts and since the only difference between the handling of straight and multibend ducts by the procedure is the difference in the transformations used, it was decided to use the experimental data taken with straight cylindrical ducts to check the procedure.

However, multibend-duct configurations were run with the procedure and checked by hand calculations to ensure that the transformations for multibend ducts would be handled properly.

The experimental data for the straight cylindrical ducts were taken by inserting aluminum ducts of different lengths and diameters through a porthole in the bottom of a 6-foot cubical tank and filling the tank with water to a level even with the top of the duct (Fig. 3). Then a source - polonium-beryllium for

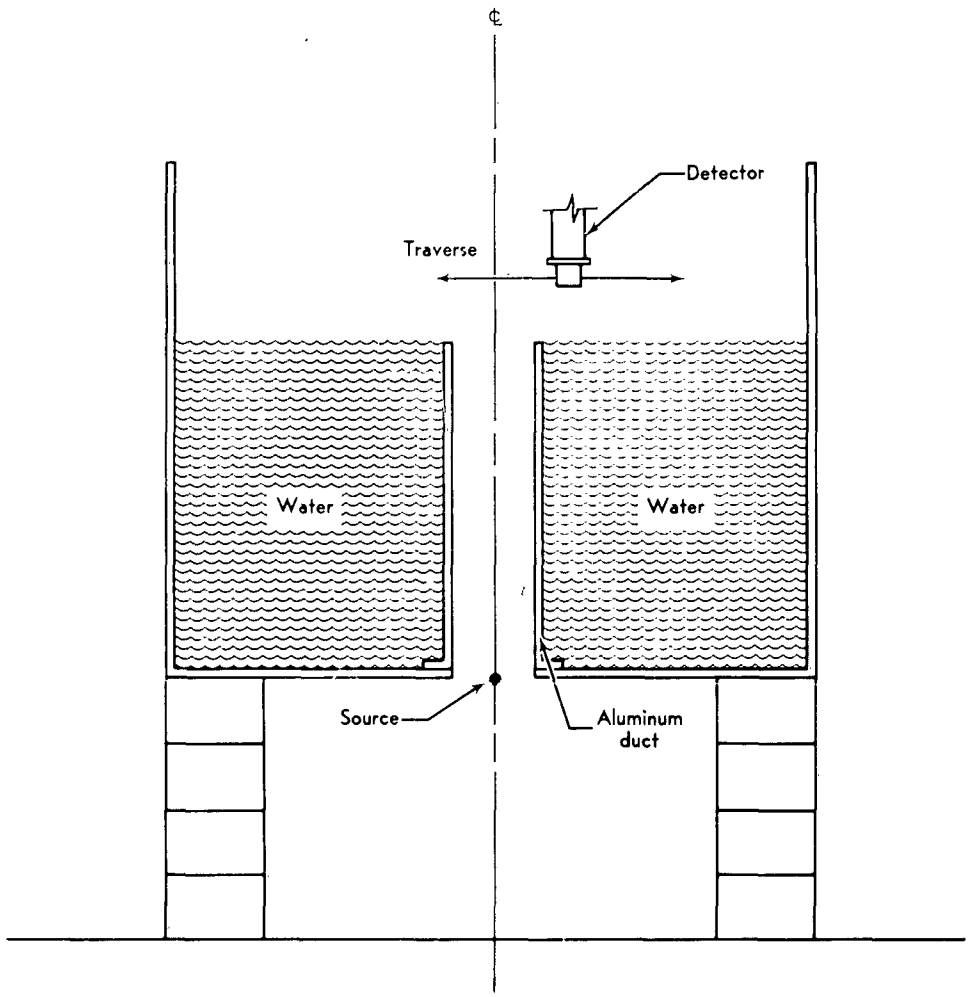

Figure 3. Experimental Setup for Duct Systemization Study

neutrons or cobalt-60 for gamma rays - was centered at the mouth of the duct, level with the bottom of the tank. The detector - a fast-neutron dosimeter (FND) for neutrons or an anthracene scintillation dosimeter (ASD) for gammas - was traversed in planes 3 inches and 15 inches above the water level. Measurements of the dose rates for the 3-inch traverse of 3-inch- and 6-inch-diameter, 12-inch-long ducts were chosen for comparison with results obtained from the multibend-duct procedure. Figures 4 and 5 show the comparison of the gamma-ray experimental and calculated data for the 3-inch traverse of a 3-inch-diameter, 12-inch-long duct and a 6-inch-diameter, 24-inch-long duct. A 444-millicurie cobalt-60 source was used in the experiment, and this source was assumed to be isotropic in the calculations.

The comparison with experimental data is somewhat better than was expected. Table I shows the statistical variations in the calculated scattered dose rates, and they became quite large as the detector point was moved farther from the centerline. There was also some question as to how well the ASD response curve and the flux-to-dose conversion curve used in the calculations would agree over the energy range considered. The energy range itself was in question, since in the calculations all photons with energies below 0.2 Mev were assumed to be absorbed. Later it was found that this was a questionable assumption, because, even though the ASD response to photons below 0.2 Mev is fairly low, there is a good possibility that if the spectrum of the scattered-

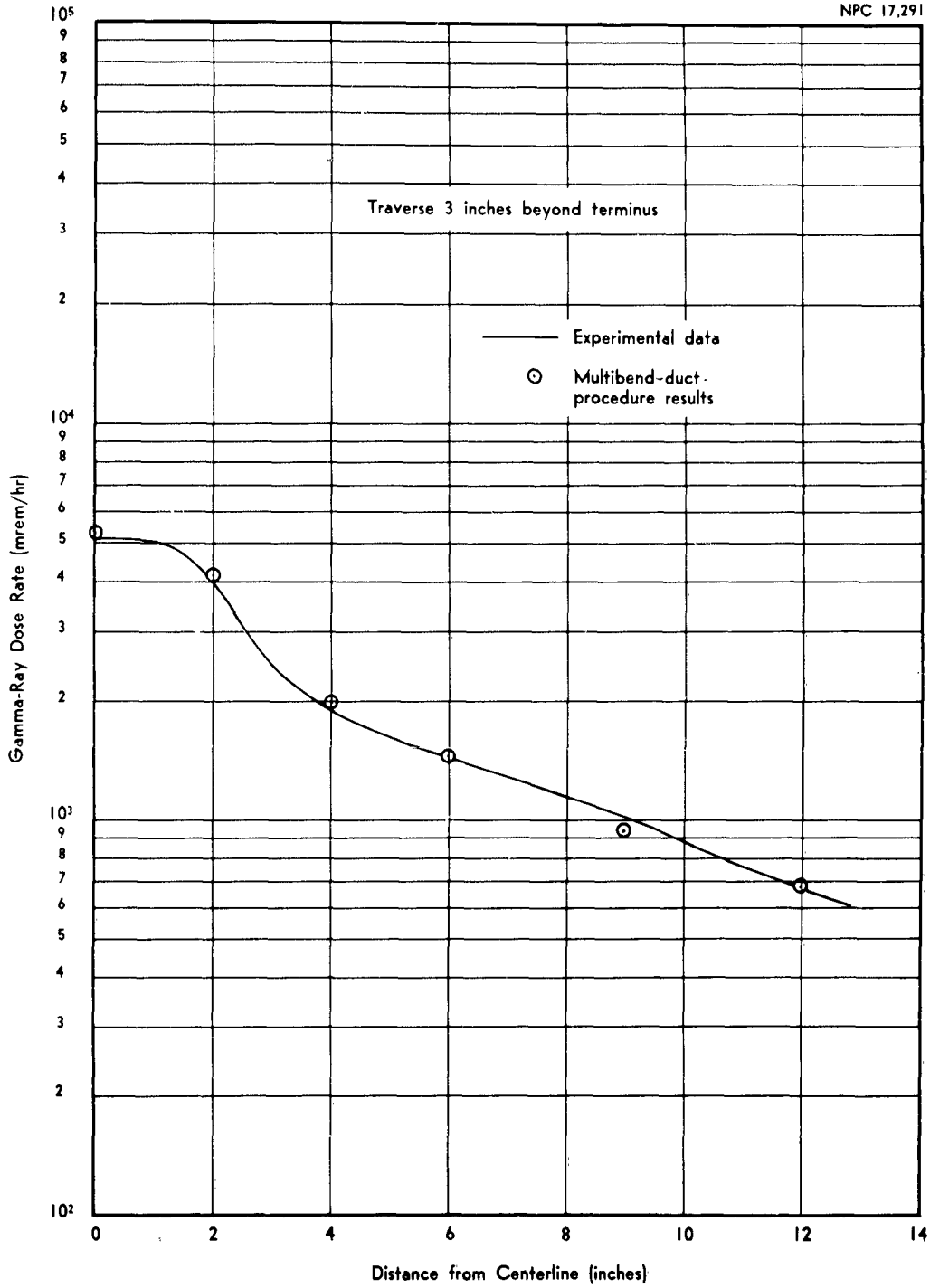

Figure 4. Comparison of Calculated and Measured Gamma-Ray Dose Rates for a 3-Inch-Diameter, 12-Inch-Long Duct

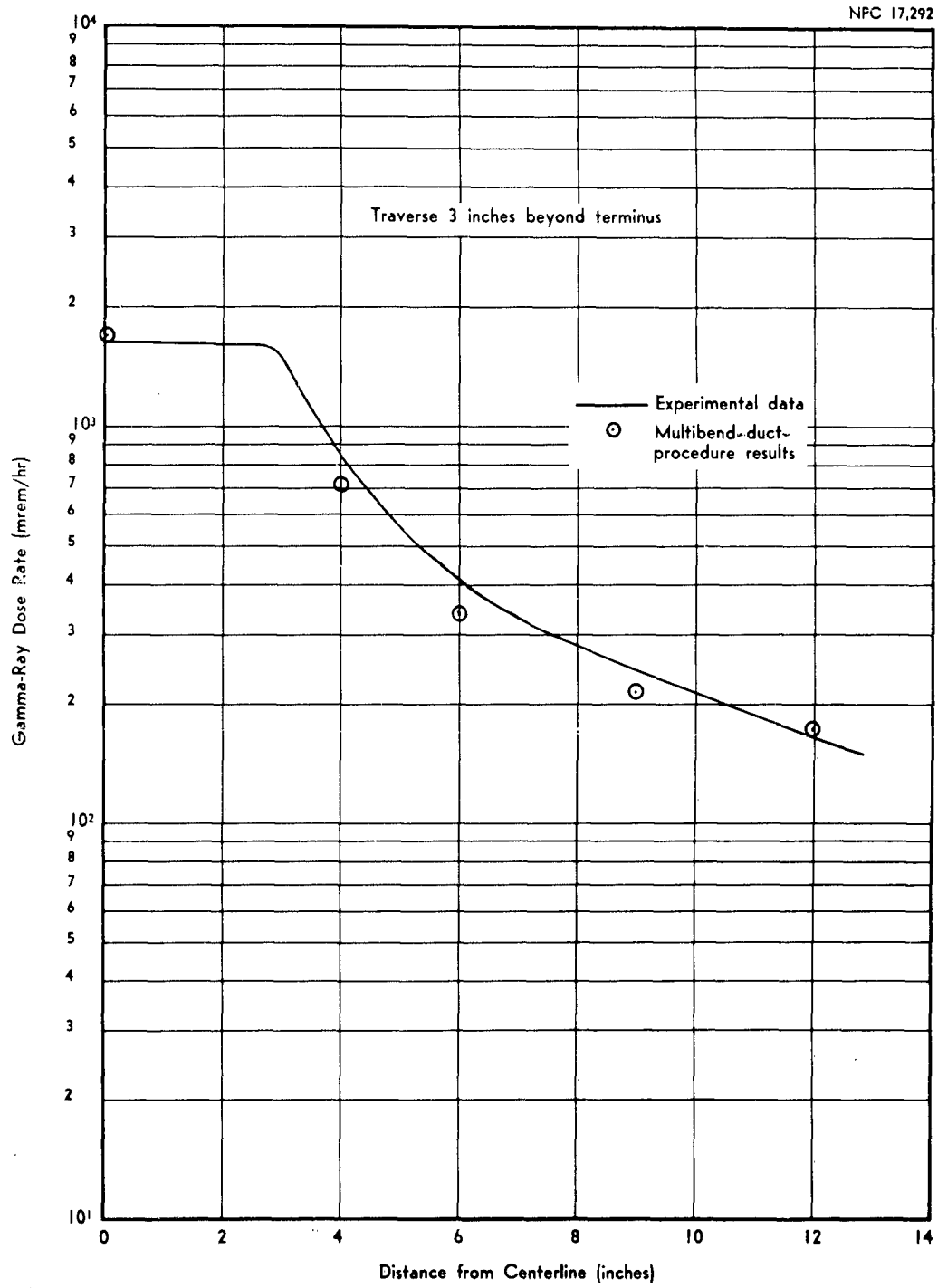

Figure 5. Comparison of Calculated and Measured Gamma-Ray Dose Rates for a 6-inch-Diameter, 24-Inch-Long Duct

TABLE I

CALCULATED COMPONENTS OF GAMMA-RAY DOSE RATES

For a 3-Inch Traverse of a 3-Inch-Diameter by 12-Inch-Long Duct and a 6-Inch-Diameter by 24-Inch-Long Duct (mrem/hr)

Distance off Centerline (inches)	3- by 12-Inch Duct			6- by 24-Inch Duct		
	Direct Beam	Scattered	Total	Direct Beam	Scattered	Total
0	4199.0	1129.9 ± 71.4	5328.9	1295.8	395.3 ± 19.8	1691.1
2	3106.5	981.4 ± 74.2	4087.9			
4	1104.6	887.8 ± 94.9	1992.4	478.4	236.9 ± 13.9	715.3
6	753.4	708.0 ± 84.8	1461.4	171.8	163.7 ± 11.6	335.5
9	470.5	480.7 ± 80.2	951.2	78.0	135.8 ± 24.7	213.8
12	293.7	401.8 ± 121.3	695.5	46.0	128.9 ± 35.3	174.9
15				29.3	89.0 ± 31.9	118.3

photon energies at the detector were known it would show a high peak in the range from 0.05 to 0.1 Mev. Measurements of the gamma-ray spectra from cobalt-60 gamma rays scattered by 1- to 12-inch-thick polyethylene slabs show a high peak at 0.1 Mev for the 1-inch slab, which gradually shifts to 0.05 Mev as the slab thickness increases to 12 inches (Ref. 7). Polyethylene and water have very similar gamma-ray attenuation properties; therefore, peaks in the 0.05- to 0.1-Mev energy range are anticipated in the scattered gamma-ray spectra at the ends of the ducts because of the scattering of the cobalt-60 gamma rays within the water surrounding the ducts. Probably some of these effects tended to cancel each other and, hence, the good agreement given in Figures 4 and 5 was obtained.

Figures 6 and 7 show the comparison of the neutron experimental and calculated data for the 3-inch traverse of both a 3-inch- and a 6-inch-diameter duct 12 inches long. A comparison with data obtained with the General Electric Flexible Monte Carlo procedure FMC-N (Ref. 8) is also presented in Figure 7. A polonium-beryllium source having a source strength of 3.98×10^7 neutrons/sec was used to obtain the experimental data for neutrons. The source angular distribution was slightly anisotropic because of the cylindrically shaped capsule containing the polonium-beryllium. The anisotrophy of the source was taken into account in the calculation of the direct-beam flux at the detector locations, but an isotropic source was assumed in the calculation of the scattered radiation.

Table II shows the scattered and unscattered components of the dose rates as calculated by the multibend procedure.

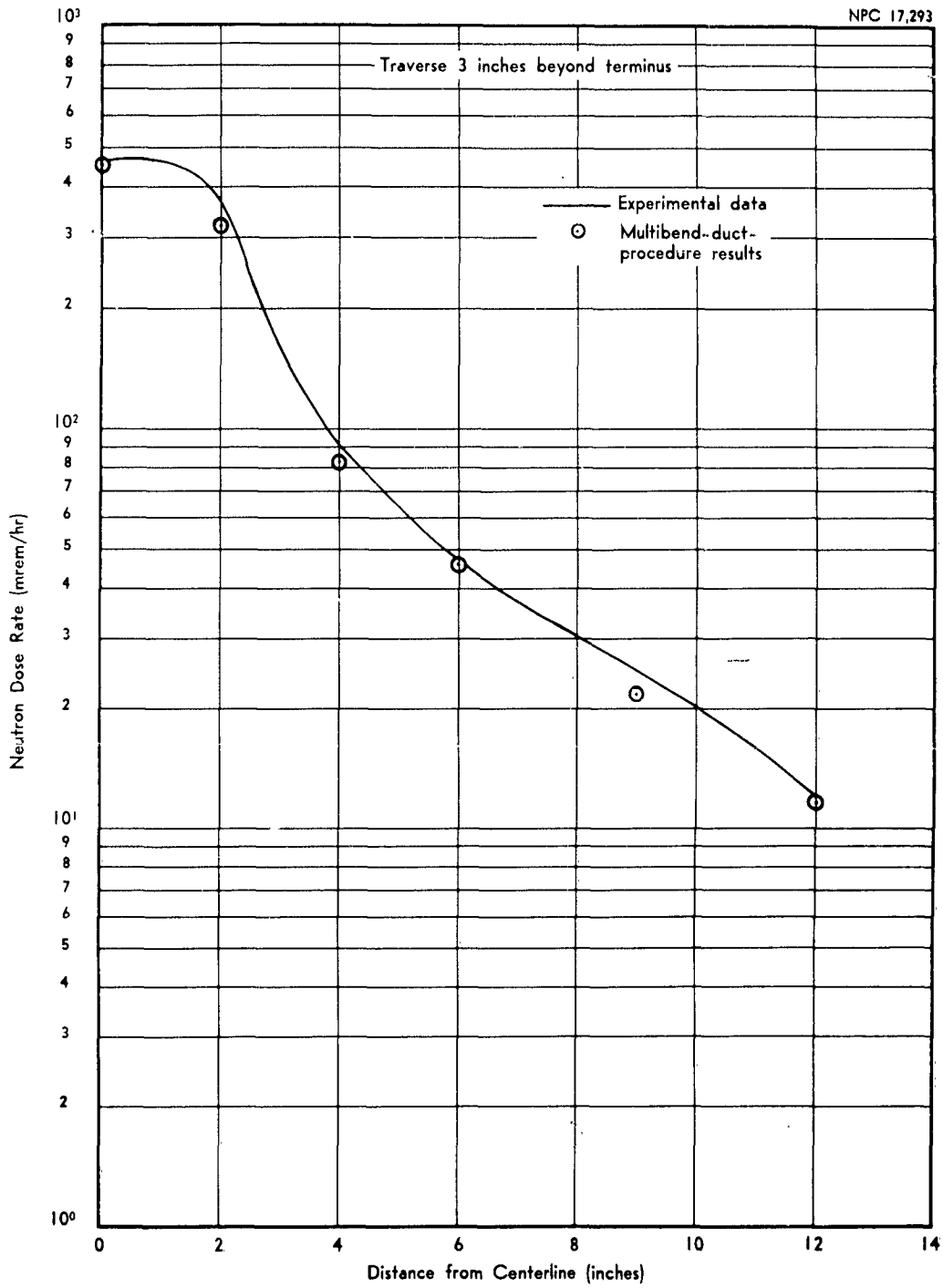

Figure 6. Comparison of Calculated and Measured Fast-Neutron Dose Rates for a 3-Inch-Diameter, 12-Inch-Long Duct

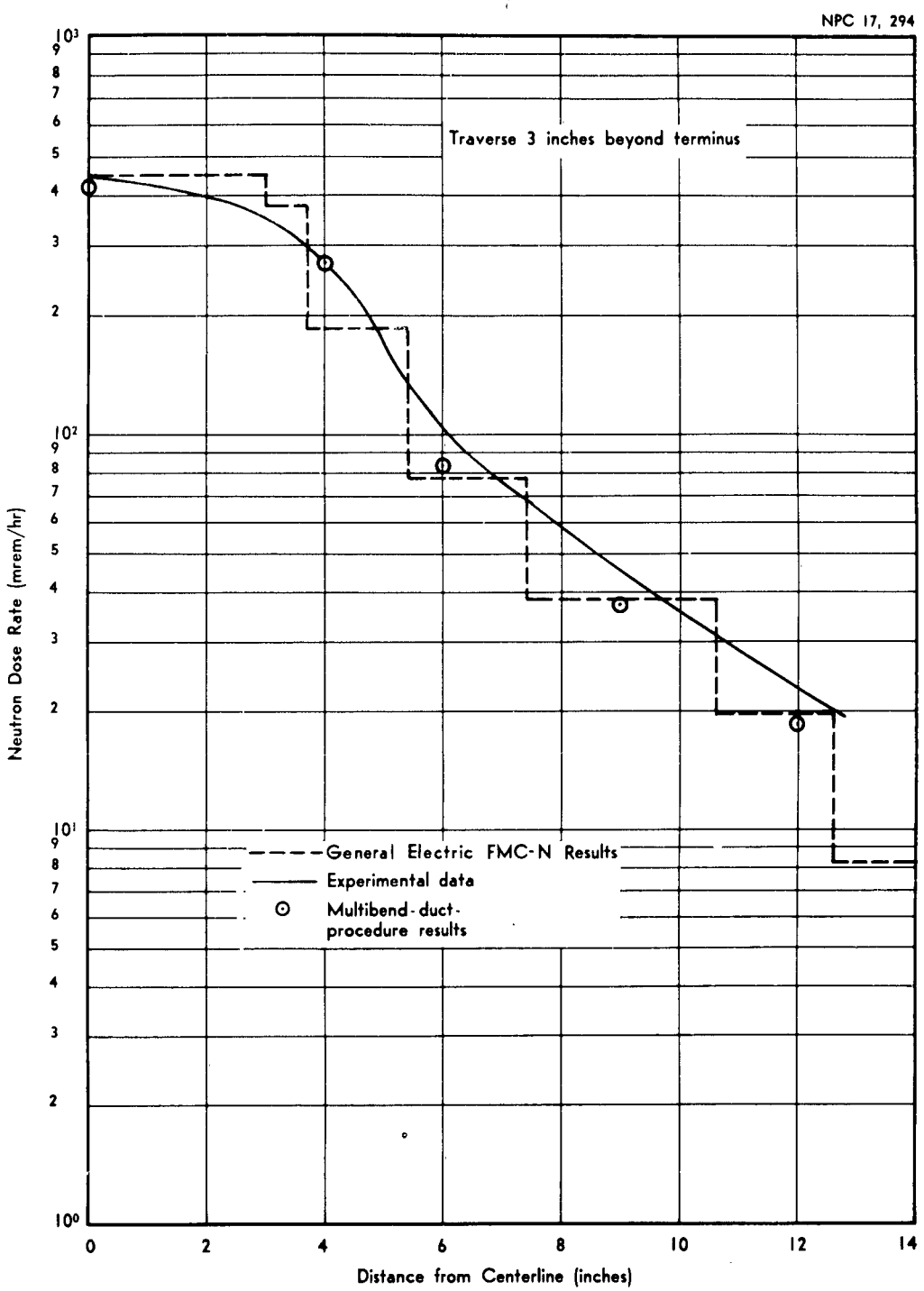

Figure 7. Comparison of Calculated and Measured Fast-Neutron Dose Rates for a 6-Inch-Diameter, 12-Inch-Long Duct

TABLE II

CALCULATED COMPONENTS OF NEUTRON DOSE RATES

For a 3-Inch Traverse of 3-Inch-Diameter by 12-Inch-Long Duct and a 6-Inch-Diameter by 12-Inch-Long Duct (mrem/hr)

Distance off Centerline (inches)	3- by 12-Inch Duct			6- by 12-Inch Duct		
	Direct Beam	Scattered	Total	Direct Beam	Scattered	Total
0	296.0	150.1 ± 10.3	446.1	296.0	110.2 ± 4.9	406.2
2	200.0	116.7 ± 9.4	316.7			
4	16.5	64.4 ± 6.9	80.9	200.0	70.3 ± 5.0	270.3
6	6.4	39.4 ± 4.4	45.8	30.0	51.1 ± 6.0	81.1
9	2.45	19.0 ± 5.9	21.5	6.2	30.8 ± 7.0	37.0
12	1.08	10.3 ± 2.7	11.4	2.5	16.1 ± 4.2	18.6

The measured FND response curve (Ref. 9) shown in Figure 8 was used in the calculations rather than a flux-to-dose conversion factor. Therefore, any disargreement with the neutron experimental data is probably due to a statistical variation in both the experimental and calculated data.

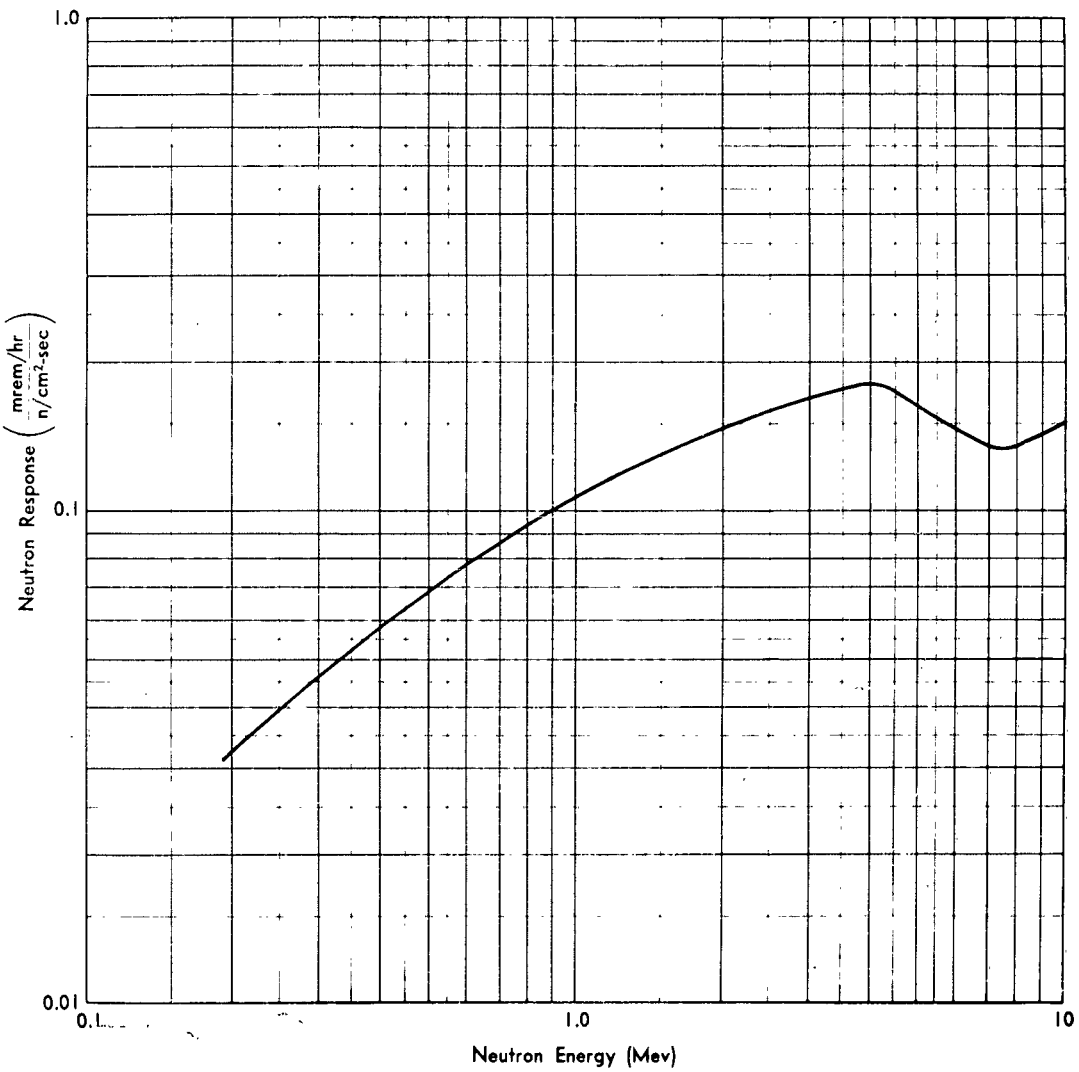

Figure 8. Fast-Neutron Dosimeter Response Curve

IV. CONCLUSIONS

In light of the good agreement obtained with experimental data for both the neutron and gamma-ray penetrations through straight cylindrical ducts and under the assumption that the application of the procedure to multibend ducts will not affect the mechanics of the calculations, it is concluded that the Multibend Duct Procedure will give an accurate prediction of neutron or gamma-ray flux penetrating a multibend duct. The ability of the procedure to treat multiple scattering rigorously and the versatility offered by the procedure in geometric description allow a fairly accurate analysis of neutron and gamma-ray radiation streaming through a multibend duct. This should lead to a more confident prediction of the flux streaming through such configurations than has been obtained with some of the less exacting methods.

It is anticipated that this procedure will be a valuable tool in the evaluation of the validity and the range of applicability of some of the simpler methods developed to calculate the amount of radiation penetrating a multibend duct.

REFERENCES

1. Simon, A., and Clifford, C. E., The Attenuation of Neutrons by Air Ducts in Shields. Oak Ridge National Laboratory Report ORNL-1217 (Revised 8 March 1954). U

2. Barcus, J. R., Transmission of Neutrons by Cylindrical Ducts Penetrating Radiation Shields. Sandia Corporation Technical Memorandum SCTM 21-59 (16) (25 March 1959). U

3. Roe, G. M., The Penetration of Neutrons through an Empty Cylindrical Duct in a Shield. Knolls Atomic Power Laboratory Report KAPL-712 (29 March 1952). U

4. Collins, D. G., A Monte Carlo Procedure for Calculating Penetration of Neutrons through Straight Cylindrical Ducts. General Dynamics/Fort Worth Report MR-N-286 (MARF-61-33T, 24 November 1961). U

5. Kahn, Herman, Applications of Monte Carlo. Rand Corporation Report RM-1237-AEC (Revised 27 April 1956). U

6. McCleary, L. W., and Collins, D. G., A Duct Systemization and Penetration Study. General Dynamics/Fort Worth Report (to be published).

7. Western, G. T., Energy Distribution of Gamma-Ray Buildup in Polyethylene Slabs. General Dynamics/Fort Worth Report FZM-2772 (28 November 1962). A paper presented at the American Nuclear Society Meeting, Washington, D. C., 6-8 November 1962.

8. Loechler, J. J., and MacDonald, J. E., Flexible Monte Carlo Programs FMC-N and FMC-G. General Electric Report APEX-706 (28 April 1961). U

9. NARF Progress Report - Shielding, 1 October 1958 through 31 March 1959. Convair-Fort Worth Report (NARF-59-18P). SRD

EXTERNAL DISTRIBUTION

MR-N-297 — 15 September 1962

Copies	Recipient
2	ASRCNL
2	ASRCPR-2
2	ASRMCE-1
2	ASRMPE-2
2	ASBMPT
1	ASTEN
3	ASAPRD-NS
1	GD/Convair
2	Convair-ASTRO
20	TIS
1	Lockheed-Ga.
1	Boeing AFPR
1	Douglas, Dept A26
1	North American
1	Pratt and Whitney
1	ORNL
1	NDA
1	Naval Ord Lab
1	Battelle-REIC
1	Air Univ Lib
1	Radioplane
1	Republic Avia
1	Vought-Aero
1	AFSWC (Tech Inf)
1	NASA-MSFC
1	NASA-Wash.
1	NASA-Lewis
1	AFPR-RCRFE
1	AFRDC-AE
1	ASRSMX-2
2	ASRKMA
1	AFSWC (SWVP)
1	TRG
10	ASTIA
2	Sandia
1	Bureau of Ships
1	DOFL (Chief-230)
1	Aerojet-General Nucleonics

Nuclear Aerospace Research Facility, General Dynamics/Fort Worth, Fort Worth, Texas. A MONTE CARLO MULTIBEND-DUCT PROCEDURE, by D. G. Collins. 15 September 1962. p. incl. illus., tables, 8 refs. (NARF-62-13T; MR-N-297)
Contract AF33(657)-7201 Unclassified report

A Monte Carlo procedure was developed to evaluate the energy, angular distribution, and intensity of either the scattered neutron or gamma-ray flux that penetrates a multibend duct. The procedure has been coded for the IBM 7090.

A detailed presentation of the Monte Carlo method as an approximation to the Neumann series solution of the integral transport equation is given. Sampling techniques utilized by the procedure are described. Included in these techniques are splitting, Russian Roulette, statistical estimation, and a method of biasing the sampling from the source angular distributions.

UNCLASSIFIED

1. Ducts, *Radiation shielding
2. *Nuclear scattering, Gamma-ray scattering, Neutron scattering
3. *Monte Carlo method, Mathematical analysis, Radiation transport
4. Nuclear physics, Nuclear physics laboratories

I. Collins, D. G.
II. Aeronautical Systems Division, Air Force Systems Command
III. Contract AF33(657)-7201

UNCLASSIFIED

Results obtained with the procedure are compared with the data taken in the duct penetration and systemization experiment conducted at General Dynamics/Fort Worth. This comparison confirms the validity of the methods. Further, it shows that the procedure will be a valuable aid in the analysis of experimental data as well as in the determination of the validity and range of applicability of some of the simpler methods developed to calculate the flux penetrating a multibend duct.

UNCLASSIFIED

Nuclear Aerospace Research Facility, General Dynamics/Fort Worth, Fort Worth, Texas. A MONTE CARLO MULTIBEND-DUCT PROCEDURE, by D. G. Collins. 15 September 1962. p. incl. illus., tables, 8 refs. (NARF-62-13T; MR-N-297)
Contract AF33(657)-7201 Unclassified report

A Monte Carlo procedure was developed to evaluate the energy, angular distribution, and intensity of either the scattered neutron or gamma-ray flux that penetrates a multibend duct. The procedure has been coded for the IBM 7090.

A detailed presentation of the Monte Carlo method as an approximation to the Neumann series solution of the integral transport equation is given. Sampling techniques utilized by the procedure are described. Included in these techniques are splitting, Russian Roulette, statistical estimation, and a method of biasing the sampling from the source angular distributions.

UNCLASSIFIED

1. Ducts, *Radiation shielding
2. *Nuclear scattering, Gamma-ray scattering, Neutron scattering
3. *Monte Carlo method, Mathematical analysis, Radiation transport
4. Nuclear physics, Nuclear physics laboratories

I. Collins, D. G.
II. Aeronautical Systems Division, Air Force Systems Command
III. Contract AF33(657)-7201

UNCLASSIFIED

Results obtained with the procedure are compared with the data taken in the duct penetration and systemization experiment conducted at General Dynamics/Fort Worth. This comparison confirms the validity of the methods. Further, it shows that the procedure will be a valuable aid in the determination of the validity and range of applicability of some of the simpler methods developed to calculate the flux penetrating a multibend duct.

UNCLASSIFIED